

Long-range orientation correlation in liquids

David P. Shelton^{a)}*Department of Physics and Astronomy, University of Nevada, Las Vegas, Nevada 89154-4002, USA*

(Received 1 December 2011; accepted 3 January 2012; published online 23 January 2012)

Strong short-range intermolecular interactions result in position and orientation correlations between nearest neighbour molecules in isotropic liquids, and it is generally assumed that such correlations extend at most a few molecular diameters. This assumption is contradicted by results from second harmonic light scattering experiments presented here, which reveal long-range orientation correlations in several isotropic liquids including water. These experiments measure the polarization dependence of the scattered light, and the observations are interpreted in terms of transverse and longitudinal polar collective modes, as well as simple explicit models. The results revise our understanding of the structure of molecular liquids and provide a test of computational simulations. © 2012 American Institute of Physics. [doi:10.1063/1.3678314]

I. INTRODUCTION

It has long been understood that the shape of molecules and short range steric effects exert the dominant influence on the local structure of liquids,¹⁻³ and it is generally assumed that the intermolecular correlations in liquids extend at most a few molecular diameters. This is in contrast to crystalline solids, where long-range periodic order is the result of the same short-range interactions, and where direct and detailed structural information is provided by x-ray, electron, and neutron diffraction measurements. However, these diffraction probes are not sensitive to long-range correlations, which may exist in systems that lack periodic positional order. A recent example of such a system is the amorphous metallic glass $\text{Ce}_{75}\text{Al}_{25}$, where long-range (1 cm) topological order was demonstrated, which was invisible to x-ray and electron diffraction.⁴ A nematic liquid crystal is another system without positional order which instead exhibits long-range orientation order for the molecules.^{2,3} The ordered domains in bulk nematic fluids cause intense light scattering due to refractive index fluctuations on the μm length scale, and the molecular orientation order can also be detected by x-ray diffraction for samples with fixed, uniform director orientation.² For the isotropic phase of nematic liquid crystals, the orientation correlations are much more difficult to measure, but orientation correlation lengths 2–10 nm have been determined using light scattering measurements for a few cases.^{5,6} Orientation correlations with range as large as 2 nm have been observed in some isotropic liquids using x-ray and neutron diffraction,⁷⁻⁹ but the usual diffraction experiments measure the pair distribution function of the single particle density averaged over the sample, and molecular orientation correlations in liquids with length scale >2 nm are nearly invisible to these probes. Measurements of higher order correlations are needed to reveal such hidden structure in disordered materials.¹⁰ Thus, in the case of isotropic liquids, one may say that there has been an absence of evidence for long-range correlations, rather than evidence for the absence of long-range correlations. The ex-

periments presented below provide evidence for long-range orientation correlation of the molecules in several isotropic liquids.

These experiments use second harmonic or hyper-Rayleigh light scattering (HRS), which is mediated by the third rank molecular hyperpolarizability β , and probes non-centrosymmetric fluctuations such as orientation fluctuations of polar molecules.¹¹⁻¹³ The present HRS measurements were made with linear polarized light at or near the 90° scattering angle, using previously described apparatus and techniques.¹³⁻¹⁵ The usual 90° scattering configurations with incident and scattered light polarized either perpendicular or parallel to the horizontal scattering plane are denoted VV, HV, VH, and HH, where V denotes vertical polarization, H denotes horizontal polarization, and the first and second letters refer to the incident and scattered light, respectively. The presence of polar collective modes and long-range molecular correlation is revealed in these experiments by the observation $I_{\text{HV}} \neq I_{\text{VH}}$ for the HRS intensities.

For liquids with uncorrelated, randomly oriented molecules the HRS intensity is the incoherent sum of local individual molecular contributions and is proportional to the isotropic average of HRS from a single molecule. The HV and VH configurations are indistinguishable for such local mode dipolar HRS, but quadrupolar HRS has a contribution proportional to the product of the electric field and field gradient of the incident light for which $I_{\text{VH}} \geq I_{\text{HV}} = 0$.¹⁶ This quadrupolar HRS has been observed for some centrosymmetric crystals where dipolar HRS is symmetry forbidden,¹⁷ but quadrupolar HRS is negligibly weak compared to dipolar HRS for molecular fluids.¹³ However, the symmetry between HV and VH can also be broken for dipolar HRS in the case that molecular orientations are correlated on a length scale comparable to the wavelength of the scattering wavevector $\mathbf{K} = 2\mathbf{k}_i - \mathbf{k}_s$, where \mathbf{k}_i and \mathbf{k}_s are the wavevectors of the incident and scattered photons, respectively. Then, the coherent sum of molecular HRS contributions has a wavevector dependence that distinguishes HV from VH and provides information about the form of the molecular correlation.

^{a)}Electronic mail: shelton@physics.unlv.edu.

TABLE I. HRS data and fit parameters for 17 molecular liquids given in order of descending I_{HV}/I_{VH} (with 1 S.D. uncertainty in the last digit shown in parenthesis). The measurements are at $T = 25.0$ °C and $\theta = 90^\circ$ except as stated. The HRS polarization ratios have been corrected for ion contamination using measured S/B , and $\Delta\theta_0$ is the deviation from the nominal 90° scattering angle. Numbers given without error bars are assumed values.

Molecule	I_{VV}/I_{HV}	I_{HV}/I_{VH}	I_{HH}/I_{VH}	S/B (%)	$\Delta\theta_0$ (deg)	A_0/A_T	A_L/A_T
CH ₃ CN	7.70(1)	1.725(8)	0.865(5) ^a 1.012(3) 1.173(4) ^b	0.0(2)	0.23(2)	0.210(2)	-0.02(1)
D ₂ O	7.38(2)	1.631(4)	0.884(4) ^a 1.006(4) 1.152(4) ^b	0.0(2)	0.15(5)	0.277(3)	0.010(5)
C ₆ F ₅ CN	6.362(6)	1.360(2)	0.935(1) ^a 1.001(1) 1.083(1) ^b	0.7(1)	0.03(2)	0.66(3)	0.12(1)
C ₆ D ₅ NO ₂	6.029(6)	1.356(1)	1.002(1)	0.7(1)	0.07(3)	0.810(2)	0.049(2)
5CB ^c	4.97(1)	1.253(3)	...	1.5(2)	0	1.159(6)	0.13(1)
C ₂ Cl ₄	3.816(7)	1.058(2)	...	0	0	2.24(1)	0.65(1)
CS ₂	3.316(4)	1.053(1)	0.998(2) ^a 0.999(1) 1.010(2) ^b	0	0	3.13(2)	0.59(2)
C ₆ D ₆	3.29(1)	1.016(3)	...	0	0	3.19(3)	0.87(3)
CCl ₄	2.107(2)	1.014(1)	1.002(1) ^a 1.001(1) 1.010(1) ^b	0.00(2)	0	11.44(5)	0.65(3)
CH ₂ Cl ₂	4.08(8)	1.00(2)	...	2(1)	0	1.9(1)	1.0(1)
CD ₃ NO ₂	3.041(6)	0.991(3)	...	1.9(2)	0	3.87(2)	1.09(3)
C ₆ F ₆	3.52(3)	0.98(1)	...	0	0	2.72(5)	1.12(7)
CD ₃ OD	6.79(4)	0.93(1)	...	2.6(5)	0	0.4(4)	1.2(12)
CDCl ₃	2.586(4)	0.929(2)	1.019(2) ^a 0.999(2) 0.993(2) ^b	0.0(2)	0.0(2)	5.90(2)	2.06(2)
Propylene carbonate	2.01(2)	0.89(2)	...	0.3(7)	0	13.7(6)	4.5(6)
(CD ₃) ₂ CO	2.797(8)	0.766(3)	...	4.8(3)	0	4.78(3)	4.54(6)
(CD ₃) ₂ SO	6.047(1)	0.637(1)	1.084(1) ^a 0.994(2) 0.946(1) ^b	1.1(1)	-0.04(8)	0.650(1)	2.88(3)

^aCell rotated $\Delta\theta' = -4^\circ$.

^bCell rotated $\Delta\theta' = +4^\circ$.

^cIsotropic phase of 4'-pentyl-4-cyanobiphenyl at $T = 38$ °C.

II. THEORY

The Cartesian hyperpolarizability tensor β_{ijk} for a molecule far from resonance has full permutation symmetry of the spatial indices (Kleinman symmetry), and $\beta = \beta^{(1)} \oplus \beta^{(3)}$ is the direct sum of first and third rank irreducible spherical tensors which contribute separately to the HRS intensity.¹¹ The HRS intensities, including contributions from randomly oriented molecules and from transverse and longitudinal polar collective modes, are given by the expressions^{12,13}

$$I_{VV} = A_0 P^2 + A_T R^2, \quad (1)$$

$$I_{HV} = A_0 + A_T, \quad (2)$$

$$I_{VH} = A_0 + A_T \sin^2(\theta/2) + A_L \cos^2(\theta/2), \quad (3)$$

$$I_{HH} = A_0[\sin^2 \theta + P^2 \cos^2 \theta] + A_T[1 - (R - 1) \cos \theta]^2 \times \sin^2(\theta/2) + A_L[1 + (R - 1) \cos \theta]^2 \cos^2(\theta/2), \quad (4)$$

where θ is the scattering angle in the horizontal plane. The irreducible third rank part of β gives terms with $P^2 = 3/2$ and intensity coefficient A_0 , while the irreducible first rank part gives terms with $R = 3$ and transverse and longitudinal intensity coefficients A_T and A_L . The HRS signal observed in a particular direction is due to the longitudinal and transverse Fourier components of the induced second harmonic polarization vector field in the medium, with wavevector equal to the scattering wavevector \mathbf{K} . For liquids with uncorrelated, randomly oriented molecules, the amplitudes of the longitudinal and transverse Fourier components are equal, and Eqs. (1)–(4) with $A_T = A_L$ reduce to just the same form as for pure local mode HRS from randomly oriented molecules, where $I_{HV} = I_{VH}$. Otherwise, $A_T \neq A_L$ resulting from molecular orientation correlation has the observable effect $I_{HV} \neq I_{VH}$.

III. EXPERIMENT

Table I shows HRS measurements for several liquids made at laser wavelength $\lambda_0 = 1064$ nm and scattering angles near 90° . The HRS polarization ratios in Table I are

extrapolated to zero collection aperture and corrected for ion contamination.¹⁵ Sample purity was >99.9%, except for nitromethane (99.7%) and perfluorobenzonitrile (99.4%). A loop containing an ion-exchange resin column was used to deionize the water and acetonitrile samples; acetone, methanol, dichloromethane, and nitromethane were distilled into the sample cell; the other samples were filled into the cell through a 0.2 μm particle filter. The narrow spike induced in the VH HRS spectrum by residual dissolved ions was measured by scanning the spectrum at 13 MHz resolution, and the ratio of integrated intensities for the spike and the broader intrinsic VH HRS spectrum is given as S/B in Table I. The corrected polarization ratios $(I_{\text{HV}}/I_{\text{VH}}) = (1 + S/B)(I_{\text{HV}}/I_{\text{VH}})_{\text{meas}}$ are given in Table I. Long-range orientation correlation is indicated, for all the liquids except dichloromethane, by a significant deviation from $I_{\text{HV}}/I_{\text{VH}} = 1$.

IV. RESULTS AND DISCUSSION

The HRS intensity coefficient ratios A_0/A_T and A_L/A_T for each liquid were obtained by fitting Eqs. (1)–(4) to the HRS polarization ratio data in Table I. The minimum data required for a fit are the values for $I_{\text{VV}}/I_{\text{HV}}$ and $I_{\text{HV}}/I_{\text{VH}}$. The measurements of $I_{\text{HH}}/I_{\text{VH}}$ made for some of the liquids also serve to test the angular dependence predicted by Eqs. (3) and (4). The scattering angle was varied by rotating the sample cell assembly and is given by $\theta = 90^\circ + \Delta\theta_0 + \Delta\theta'/n$, where $\Delta\theta_0$ is the deviation from the nominal 90° scattering angle, $\Delta\theta'$ is the cell rotation angle, and n is the sample refractive index at the laser wavelength.¹⁸ Kleinman symmetry and the value $R = 3$ were assumed for the fits, except for nitrobenzene where the previously determined value $R = 3.114$ was used,¹³ and perfluorobenzonitrile where $R = 3.10 \pm 0.02$ was needed to adequately fit the present data. The ratio A_0/A_T indicates the relative strength of the octupolar $\beta^{(3)}$ HRS contribution, and is largest for CCl_4 . The ratio A_L/A_T in Table I indicates the type of orientation correlation, which ranges from a nearly pure transverse mode with $A_L/A_T \approx 0$ for acetonitrile and water, to a dominant longitudinal mode with $A_L/A_T > 4$ for acetone and propylene carbonate. Significant correlations are seen even for several liquids with centrosymmetric molecules. In these liquids, the $\beta^{(1)}$ contribution (which reports the orientation correlations) is induced by distortion of a given molecule by the multipole fields of neighbouring molecules in close collisions.¹⁹ The slope of $I_{\text{HH}}/I_{\text{VH}}$ as a function of θ at $\theta = 90^\circ$ is also a clear indication of long-range correlations, with a positive slope when transverse modes dominate, a negative slope when longitudinal modes dominate, and zero slope for local modes. Figure 1 shows that there is good agreement between the data and fitted curves for $I_{\text{HH}}/I_{\text{VH}}$ versus θ .

The results in Table I indicate long-range correlations in essentially every case, with strong transverse mode HRS observed more frequently than strong longitudinal mode HRS, but the strength and range of the molecular correlations are undetermined. The form of the correlation is known for the previously studied example of pure longitudinal mode HRS induced by the radial electric field around a dissolved ion.²⁰ The ion electric field orients and distorts the molecules in the liquid, producing a radial orientation alignment of the sur-

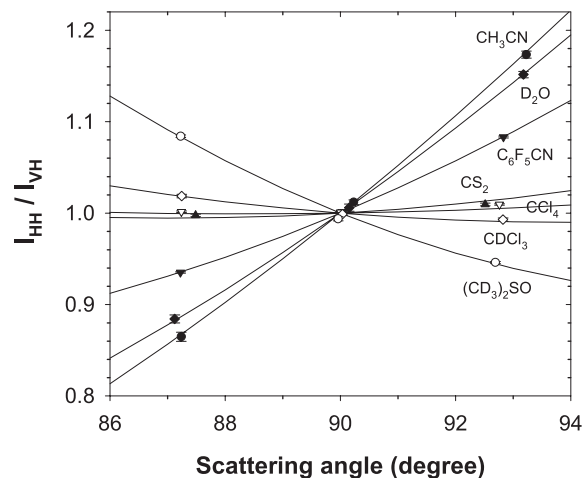


FIG. 1. Data (symbols) and theoretical fits (curves) for $I_{\text{HH}}/I_{\text{VH}}$ versus scattering angle are compared for several molecular liquids. Local mode HRS gives zero slope at $\theta = 90^\circ$.

rounding molecules that falls off as r^{-2} , with the main longitudinal mode HRS contribution coming from the molecules in a spherical volume with 140 nm radius. This example suggests a simple model for molecular correlations that could produce intrinsic longitudinal mode HRS in a liquid. The model has spherical domains with radius r_0 , where fraction A of the molecules is radially oriented with their polar z axis pointing outward, and where the remaining $(1 - A)$ molecules are randomly oriented. It is further assumed that the molecular hyperpolarizability is one-dimensional so that β_{zzz} is the only non-zero component of β . In this case, the second harmonic dipole points along the molecular z axis and is proportional to the square of the applied field component along the molecular z axis. For this model (at $\theta = 90^\circ$), one obtains $I_{\text{VV}}/I_{\text{HV}} = 5$ and

$$I_{\text{HV}}/I_{\text{VH}} = [1 + g_L(A, x_0)]^{-1}, \quad (5)$$

where

$$g_L(A, x_0) = \frac{105}{4\pi^2} \frac{A^2}{1-A} \frac{\rho \Lambda^3}{x_0^3} \left[\frac{3 \sin x_0}{x_0} - \cos x_0 - 2 \right]^2, \quad (6)$$

$x_0 = Kr_0$ is the scaled domain radius, $\Lambda = 2\pi/K \approx \lambda_0/(2n\sqrt{2})$ is the wavelength for the Fourier component contributing to the HRS signal, ρ is the molecular number density, λ_0 is the vacuum wavelength of the incident light, and n is the refractive index of the liquid. The relative longitudinal mode contribution increases as $g_L(A, x_0) \propto x_0^5$ for small x_0 , and reaches its maximum at $x_0 \approx 4.75$.

This simple model has been used to estimate the strength and range of the molecular correlations in $(\text{CD}_3)_2\text{SO}$ (DMSO). The observed value $I_{\text{VV}}/I_{\text{HV}} = 6.047$ for DMSO is close to the value $I_{\text{VV}}/I_{\text{HV}} = 5$ for this model, and the observed values $I_{\text{HV}}/I_{\text{VH}} = 0.637$ and $g_L = 0.57$ for DMSO indicate a predominant longitudinal mode contribution. Figure 2 shows $g_L(A, x_0)$ evaluated using $\rho = 14 \text{ M} = 8.5 \text{ nm}^{-3}$ and $\Lambda = 256 \text{ nm}$ for DMSO. The estimated domain radius which gives $g_L = 0.57$ depends on the correlated fraction of molecules, with values $r_0 = 3, 5, 9, 23, 59 \text{ nm}$ for $A = 80\%$,

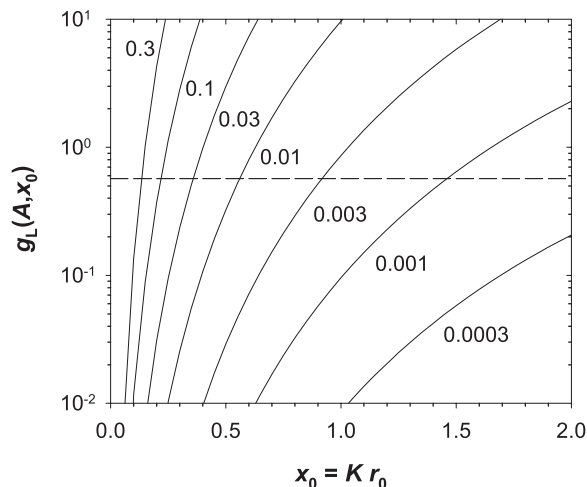


FIG. 2. Model calculation for HRS from a spherical domain with radius r_0 , containing radially polarized molecular fraction A (of 1D chromophores). The curves, labelled by the value of A , are the function $g_L(A, x_0) = (I_{HV}/I_{VH})^{-1} - 1$, which indicates the strength of the longitudinal mode HRS contribution. For DMSO-d₆, the observed value is $g_L = 0.57$ (horizontal dashed line), and the length scale is $K^{-1} = 41$ nm.

40%, 10%, 1%, 0.1%, respectively. The smallest A for which $g_L = 0.57$ can be obtained using this model is $A = 0.015\%$ with $r_0 = 193$ nm. These results indicate a lower bound near 3 nm for the radius of the correlated domains, but then a very high degree of polar molecular orientation order would have to exist. Domains with correlation length >10 nm would require a much smaller polar aligned fraction A of molecules to account for the HRS observations. The polar correlations in this model are not inconsistent with the results of neutron scattering experiments for DMSO, which find antiparallel dipole correlation for nearest neighbour molecules and parallel dipole correlation at larger distance.⁸ The model can agree with these results if nearly equal numbers of outward and inward radially pointing molecules are mixed together, with a small excess of outward pointing molecules constituting the net outward polar aligned fraction A , so that the local correlation is antiparallel, but at longer range the correlation is parallel.

A simple model for molecular correlations which can produce transverse mode HRS has spherical domains with radius r_0 , where fraction A of the molecules point azimuthally (e.g., clockwise) around an axis through the center of the domain, and where the remaining $(1 - A)$ molecules are randomly oriented. It is also assumed that the individual domains are randomly oriented, and that the molecular hyperpolarizability is one-dimensional so that β_{zzz} is the only non-zero component of β . For this model (at $\theta = 90^\circ$, for small x_0), one obtains

$$I_{VV}/I_{HV} = \frac{[5 + 216 g_T(A, x_0)]}{[1 + 30 g_T(A, x_0)]}, \quad (7)$$

$$I_{HV}/I_{VH} = \frac{[1 + 30 g_T(A, x_0)]}{[1 + 20 g_T(A, x_0)]}, \quad (8)$$

where

$$g_T(A, x_0) = \frac{A^2}{1 - A} \frac{\rho \Lambda^3}{8^5} x_0^5. \quad (9)$$

This model fits the observed result $I_{HV}/I_{VH} = 1.356$ for nitrobenzene, using the parameter values $\rho = 10 \text{ M} = 6 \text{ nm}^{-3}$ and $\Lambda = 246$ nm, with $r_0 = 5, 10, 20$ nm and $A = 46\%, 12\%, 2\%$, respectively. The model also gives $I_{VV}/I_{HV} = 6.14$ as compared to the observed value 6.03 for nitrobenzene. However, for this simple model, the possible values $I_{VV}/I_{HV} \leq 7.2$ and $I_{HV}/I_{VH} \leq 1.5$ are too small to fit the observations for water and acetonitrile, which indicates that the model needs to incorporate a more realistic hyperpolarizability tensor for these molecules.

Further evidence for a correlation length longer than 5 nm comes from a previous HRS experiment, where A_L/A_T was measured for nitrobenzene as the nitrobenzene was diluted with benzene.²¹ The nitrobenzene HRS signal has the polarization signature of a nearly pure transverse mode even at 1000-fold dilution, which indicates that the nitrobenzene polar correlation has not decreased at 5.5 nm intermolecular separation. It appears as if the long-range orientation correlations in the dilute solution are carried by the benzene molecules and are merely reported by the embedded nitrobenzene molecules. This is consistent with the result $A_L/A_T = 0.87$ observed for pure benzene in the present experiment, which indicates significant long-range transverse orientation correlation for the benzene molecules. HRS from the centrosymmetric benzene molecules is due to the transient β induced in a benzene molecule by the quadrupole electric field of a colliding neighbour molecule.¹⁹ Since induced β is not rigidly aligned along a molecular axis, a weak HRS transverse mode signature may result in spite of strong orientation correlation of the molecules. For C_6F_6 , the values for both the molecular quadrupole moment²² and $A_L/A_T - 1$ have the same magnitude but opposite sign as compared to the corresponding values for C_6D_6 .

Based on the above experiments, the correlated domains are estimated to have radius > 5 nm and contain >5000 molecules. Molecular dynamics simulations have the potential to provide the most direct and detailed information about molecular correlations and liquid structure, but there are few molecular dynamics simulations with such large scale, using realistic intermolecular potentials, investigating long-range orientation correlations in molecular liquids. The recent relevant simulations include a simulation of acetonitrile with 28 000 molecules in a 13 nm box,²³ and simulations of water with 110 592 molecules in a 15 nm box,²⁴ 40 000 molecules in a 12 nm box,²⁵ and 1728 molecules in a 4 nm box.²⁶ Correlations with the range and strength suggested by the HRS experiments are not seen in the simulations. The longest dipole correlation length found in these simulations is 2.4 nm.²⁴ It is possible that long-range correlations consistent with the HRS results were present but were not detected in the analysis of the simulation results, or that they were absent due to the limited maximum length and time scales accessible in the simulations, but the apparent disagreement between the HRS experiments and the simulations needs further investigation.

V. SUMMARY

HRS was measured from isotropic liquids composed of polar or nonpolar molecules, and the experimental results

indicate long-range orientation correlation of the molecules in 16 of 17 liquids investigated. However, the strength of the HRS non-local polar mode signal does not uniquely determine the form and range of the molecular orientation correlation. The form of the orientation correlation was explored by constructing simple explicit models that can account for longitudinal or transverse polar mode HRS and applying them to analyze the DMSO and nitrobenzene observations. Based on the HRS experimental results, the estimated range of molecular orientation correlations is >5 nm. The proposed models for these liquids are spatially inhomogeneous, with domains larger than 10 nm diameter in which there is orientation order of the molecules.

¹D. Chandler, *Acc. Chem. Res.* **7**, 246 (1974).

²P. M. Chaikin and T. C. Lubensky, *Principles of Condensed Matter Physics* (Cambridge University Press, Cambridge, England, 1995).

³J.-L. Barrat and J.-P. Hansen, *Basic Concepts for Simple and Complex Liquids* (Cambridge University Press, Cambridge, England, 2003).

⁴Q. Zeng, H. Sheng, Y. Ding, L. Wang, W. Yang, J.-Z. Jiang, W. L. Mao, and H.-K. Mao, *Science* **332**, 1404 (2011).

⁵J. J. Krich, M. B. Romanowsky, and P. J. Collings, *Phys. Rev. E* **71**, 051712 (2005).

⁶E. Gulari and B. Chu, *J. Chem. Phys.* **62**, 798 (1975).

⁷S. Pothoczki, L. Temleitner, P. Jovari, S. Kohara, and L. Pusztai, *J. Chem. Phys.* **130**, 064503 (2009).

⁸S. E. McLain, A. K. Soper, and A. Luzar, *J. Chem. Phys.* **124**, 074502 (2006).

⁹N. Veglio, F. J. Bermejo, L. C. Pardo, J. Ll. Tamarit, and G. C. Cuello, *Phys. Rev. E* **72**, 031502 (2005).

¹⁰P. Wochner, C. Gutt, T. Autenrieth, T. Demmer, V. Bugaev, A. D. Ortiz, A. Duri, F. Aontone, G. Grubel, and H. Dosch, *Proc. Natl. Acad. Sci. U.S.A.* **106**, 11511 (2009).

¹¹P. D. Maker, *Phys. Rev. A* **1**, 923 (1970).

¹²D. P. Shelton, *J. Opt. Soc. Am. B* **17**, 2032 (2000).

¹³D. P. Shelton, *J. Chem. Phys.* **132**, 154506 (2010).

¹⁴D. P. Shelton, W. M. O'Donnell, and J. L. Norton, *Rev. Sci. Instrum.* **82**, 036103 (2011).

¹⁵D. P. Shelton, *Rev. Sci. Instrum.* **82**, 113103 (2011).

¹⁶S. Kielich, M. Kozierowski, A. Ozgo, and R. Zawodny, *Acta Phys. Pol.* **A45**, 9 (1974).

¹⁷V. N. Denisov, B. N. Mavrin, and V. B. Podobedov, *Phys. Rep.* **151**, 1 (1987).

¹⁸D. P. Shelton, *Appl. Opt.* **50**, 4091 (2011).

¹⁹S. Kielich, J. R. Lallane, and F. B. Martin, *Phys. Rev. Lett.* **26**, 1295 (1971).

²⁰D. P. Shelton, *J. Chem. Phys.* **130**, 114501 (2009).

²¹D. P. Shelton, *J. Chem. Phys.* **133**, 234507 (2010).

²²J. Vrbancich and G. L. D. Ritchie, *J. Chem. Soc., Faraday Trans. 2* **76**, 648 (1980).

²³M. A. Pounds and P. A. Madden, *J. Chem. Phys.* **126**, 104506 (2007).

²⁴J. M. P. Kanth, S. Vemparala, and R. Anishetty, *Phys. Rev. E* **81**, 021201 (2010).

²⁵G. Mathias and P. Tavan, *J. Chem. Phys.* **120**, 4393 (2004).

²⁶P. Kumar, G. Franzese, S. Buldyrev, and E. Stanley, *Phys. Rev. E* **73**, 041505 (2006).